Title
Exploring matrix effects on photochemistry of organic aerosols

Journal
Proceedings of the National Academy of Sciences of the United States of America, 111(38)

ISSN
0027-8424

Authors
Lignell, H
Hinks, ML
Nizkorodov, SA

Publication Date
2014-09-23

DOI
10.1073/pnas.1322106111

Exploring matrix effects on photochemistry of organic aerosols

Hanna Lignell[a,b,1], Mallory L. Hinks[a], and Sergey A. Nizkorodov[a,2]

[a]Department of Chemistry, University of California, Irvine, CA 92697-2025; and [b]Laboratory of Physical Chemistry, University of Helsinki, FIN-00014, Helsinki, Finland

Edited by Mark H. Thiemens, University of California, San Diego, La Jolla, CA, and approved August 1, 2014 (received for review November 25, 2013)

This work explores the effect of the environment on the rate of photolysis of 2,4-dinitrophenol (24-DNP), an important environmental toxin. In stark contrast to the slow photolysis of 24-DNP in an aqueous solution, the photolysis rate is increased by more than an order of magnitude for 24-DNP dissolved in 1-octanol or embedded in secondary organic material (SOM) produced by ozonolysis of α-pinene. Lowering the temperature decreased the photolysis rate of 24-DNP in SOM much more significantly than that of 24-DNP in octanol, with effective activation energies of 53 kJ/mol and 12 kJ/mol, respectively. We discuss the possibility that the increasing viscosity of the SOM matrix constrains the molecular motion, thereby suppressing the hydrogen atom transfer reaction to the photoexcited 24-DNP. This is, to our knowledge, the first report of a significant effect of the matrix, and possibly viscosity, on the rate of an atmospheric photochemical reaction within SOM. It suggests that rates of photochemical processes in organic aerosols will depend on both relative humidity and temperature and thus altitude. The results further suggest that photochemistry in SOM may play a key role in transformations of atmospheric organics. For example, 24-DNP and other nitro-aromatic compounds should readily photodegrade in organic particulate matter, which has important consequences for predicting their environmental fates and impacts.

aerosol aging | particle viscosity | organic photochemistry

Aqueous droplets and aerosol particles provide unique reaction media for complex atmospheric chemistry, and the importance of such reactions has been discussed in the literature (1, 2). Our level of understanding of chemistry occurring in gas-phase and in dilute aqueous solutions characteristic of cloud and fog droplets is relatively high. In contrast, reactions happening in/on aerosol particles are poorly understood because they possess a large degree of chemical and physical heterogeneity and the individual particle components deviate significantly from ideal behavior. Secondary organic material (SOM), which is believed to be the dominant component of atmospheric particles, especially in areas dominated by secondary organic aerosols (SOA), provides a rich environment for atmospheric chemistry and photochemistry. In this paper, the term SOM is used to refer to a condensed "organic phase" environment to distinguish it from the gas-phase and aqueous phase environments. SOA has the usual meaning of an organic aerosol produced by secondary chemistry in the atmosphere. Most of the oxidized organic compounds found in SOM have not been isolated in pure form, but based on their chemical structures, one would expect SOM to adopt a viscous liquid or solid-like phase under room temperature conditions (3). A "phase state" of SOM, which may include thousands of different compounds, is not a well-defined quantity, but it is certainly appropriate to discuss rheological properties of SOM such as its viscosity (4). The viscosity can potentially affect the dynamics of particle growth (5), the gas–particle exchange rates (6), the rate of diffusion of water (7) and oxidants through the particle (8), the dynamics of coagulation of different particles (9), reactive uptake on the particle surfaces (10, 11), etc. For example, the molecular diffusion limitations within SOM have been shown to impact particle growth mechanisms and rates (5, 12), and also affect the oxidation rates of organic constituents trapped in the particles (3, 8). Presence of water vapor has an especially strong effect on SOM viscosity by affecting volatile organic compound oxidation chemistry during the SOM formation stage (13) and by acting as an efficient plasticizer for SOM (7). It was previously assumed that SOM can be described as a "liquid" (in a sense that the timescale for diffusive mixing inside a particle is not a rate-limiting step), and that oxidation products of volatile organic compounds always adopt gas–particle partitioning equilibrium (14–16). However, it has recently been shown that the equilibration timescale for the gas–particle partitioning can range from hours to days for organic aerosol material associated with semisolid particles, especially under the conditions of large particle sizes and low aerosol mass loadings (17). The slow equilibration conditions are likely relevant in remote forest areas, where aerosol mass concentrations are relatively low and particles demonstrate amorphous solid behavior (18), and in the vicinity of tropopause, where SOM is suggested to go through glass transition because of the reduced temperatures (3).

The goal of this work is to examine the differences in photochemical behavior of atmospherically relevant organic molecules in the aqueous, liquid organic, and solid organic phases. Although the role of the environment in photochemical reactions is a subject that is as old as photochemistry itself, only a few studies in the past have systematically examined the role of organic phase in atmospheric photochemistry. The best example of this is perhaps the study by McDow et al., which analyzed the rate of photodegradation of benz[a]anthracene in several major organic compound classes believed to exist in particulate matter and observed significant differences in the photodegradation rates (19). The

Significance

Recent discovery of highly viscous materials in organic aerosols prompted atmospheric scientists to reevaluate their views of organic particle growth and chemical aging. This work reveals dramatic differences in the effect of temperature on photolysis efficiency of organic compounds trapped in viscous organic matrix, in a liquid organic solvent, and in an aqueous solution. Given the paramount role of photochemistry in driving the chemical reactions in the environment, these results will have significant implications for predicting lifetimes of photolabile atmospheric organic compounds, including environmental toxins, trapped in organic particles. This work also demonstrates that changing from water to an organic solvent can drastically enhance photochemical activity of environmental toxins, thus underscoring the importance of particle-phase photochemistry.

Author contributions: H.L. and S.A.N. designed research; H.L. and M.L.H. performed research; H.L. and M.L.H. analyzed data; and H.L., M.L.H., and S.A.N. wrote the paper.

The authors declare no conflict of interest.

This article is a PNAS Direct Submission.

[1]Present address: Division of Chemistry and Chemical Engineering, California Institute of Technology, Pasadena, CA 91125.

[2]To whom correspondence should be addressed. Email: nizkorod@uci.edu.

This article contains supporting information online at www.pnas.org/lookup/suppl/doi:10.1073/pnas.1322106111/-/DCSupplemental.

current work relies on a similar approach to investigate photochemistry of an atmospherically relevant probe molecule in multiple phases at different temperatures, specifically in water, octanol, and a surrogate SOM prepared by oxidation of α-pinene (the detailed experimental procedure is described in the *SI Appendix* text, with the help of *SI Appendix*, Figs. S1–S9). The temperature affects condensed-phase photochemistry both directly, by slowing down unimolecular decomposition and bimolecular reactions of photoexcited molecules, and indirectly, by physically changing the SOM matrix. One probable contributor to the physical changes is viscosity, which could affect the photolysis rates by constraining the motion of the molecules trapped in it. This can potentially change the yields and branching ratios of the photolytic processes occurring in the SOM matrix, by hindering intramolecular isomerization and intermolecular reactions of the electronically excited molecules or by more efficient caging of the primary photolysis products. The effect of temperature on photochemistry in a liquid is expected to be smaller than in a comparable solid. Our hypothesis is that we can decouple the direct and indirect effects of temperature by comparing photochemistry of a carefully chosen probe molecule in SOM and in an octanol film. Octanol (freezing point = −16 °C) is a relatively viscous liquid, but it is considerably less viscous than α-pinene SOM, thus potentially providing a good reference for these photochemical measurements. As a side note, octanol is commonly used in water–organic phase partitioning studies, with octanol partitioning coefficients known for a wide range of compounds, and is thought of as a "prototypical organic phase" in environmental studies (20).

The photochemical probe molecule selected for this study is 2,4-dinitrophenol (hereafter referred to as 24-DNP), a toxic nitroaromatic compound that is present in both surface waters and the atmospheric condensed phases (clouds, fogs, aerosols); 24-DNP is the most phytotoxic nitrophenol that is present in the environment to a significant extent (21), and its sources are mainly pesticide runoff to water and air pollution from manufacturing plants (22). The reasonably high water solubility (0.6 g per 100 mL at 18 °C), low vapor pressure (1.42×10^{-7} mmHg, from Environmental Protection Agency's Assessment Tools for the Evaluation of Risk Database) and high octanol–water partition coefficient (K_{ow} = 8738) (23) of 24-DNP suggest that it is as likely to be found in particulate organic phase as in water. Indeed, nitrophenols are commonly found in fog waters and make a dominant contribution to near-UV light-absorbance by aerosols (24). The importance of 24-DNP in seawater and its direct photodegradation in aqueous solutions by simulated sunlight has been studied (25, 26). The photoproducts of 24-DNP are not known, but the initial steps in the photolysis mechanism can be predicted based on the known photochemistry of mononitrophenols (27–29). What makes 24-DNP a convenient probe molecule for investigating matrix effects in photochemistry is that 24-DNP photodegradation involves a hydrogen atom transfer reaction between a long-lived electronically excited state of 24-DNP and the solvent. Constraining 24-DNP in a viscous SOM environment may therefore be expected to significantly hinder its photochemical loss.

Results and Discussion

Photolysis of 24-DNP in Different Matrices. The spectra of 24-DNP taken during the course of its photolysis in an octanol film at 25 °C are shown in Fig. 1*A*, and Fig. 1*A*, *Inset* shows the corresponding decay of the absorbance at 290 nm, where the molecular form of 24-DNP absorbs strongly. The increase in the visible absorbance (~400 nm) is indicative of the formation of a chromophoric product accompanied by a relatively strong, visually observable change in the film color. While the increased visible absorbance is worthy of note, it cannot be converted into a physically meaningful photolysis rate constant because the extinction coefficients and yields of the 24-DNP photolysis products are unknown. In contrast, the absorbance at 290 nm should be dominated by 24-DNP in the limit of low photolysis times, and it can be used to infer the photolysis rate constant as described below.

As products of the 24-DNP photolysis are unknown, we have to make simplifying assumptions about their contribution to the observed absorption spectrum to analyze the data. The simplest assumption that can be made under the circumstances is that there is a single absorbing product that does not undergo secondary photolysis. This assumption is justified by the observation of an isosbestic-like point at 340 nm in Fig. 1*A*. The normalized base-10 absorbance should then decay as follows:

$$\frac{A(t)}{A_0} = \beta + (1-\beta)\cdot e^{-kt} \qquad [1]$$

where β and k are fitting parameters. The physical meaning of parameter β is the ratio of the 290-nm molar extinction coefficient of the photolysis product to that of 24-DNP. This model predicts an exponential decay of the normalized absorbance to

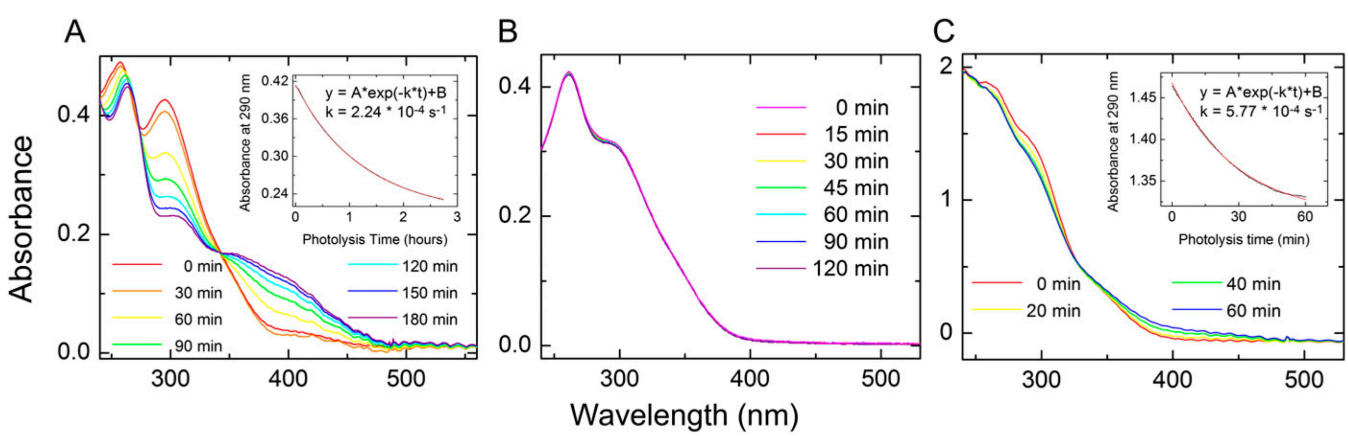

Fig. 1. Spectra measured at different times during photolysis of 24-DNP dispersed in: (*A*) octanol, (*B*) water, and (*C*) SOM matrix. *Insets* in *A* and *C* show exponential fits to the 290-nm absorbance as a function of time using Eq. **1**. In the case of photolysis in octanol and water, the photolysis rate constants can be converted into photolysis quantum yields using actinometry, as described in *SI Appendix*. Such a conversion is not possible for the photolysis in SOM, but the photolysis rate constants in SOM and octanol can be directly compared. Similar experiments were carried out at lower temperature with the working hypothesis that viscosity of octanol should be affected by the temperature much less than that of the SOM film. The temperature-dependent rate constants and quantum yields are compiled in Table 1.

an asymptotic value of β. The observed absorbance decay rates in liquid octanol films in the temperature range from −17 °C to 25 °C could be well fitted to this model; the resulting values of k and their uncertainties are listed in Table 1 and shown in Fig. 2 in the form of an Arrhenius plot. Only a weak trend in k was observed as the temperature was decreased.

The effective quantum yields of photolysis were obtained using the following equation:

$$k = \phi \int_{\lambda} \sigma(\lambda) F(\lambda) d\lambda \qquad [2]$$

where $\langle \phi \rangle$ is the quantum yield averaged over the wavelength range of the photolysis source (280–400 nm), $\sigma(\lambda)$ is the base-e absorption cross section calculated from the measured extinction coefficient of 24-DNP in octanol, and $F(\lambda)$ is the spectral flux density of the photolysis source, which was quantified using azoxybenzene actinometry carried out under identical experimental conditions (*SI Appendix*, Fig. S4). A detailed treatment of the equations and assumptions related to the actinometry and quantum yield calculations can be found in ref. 30. The resulting quantum yields are on the order of 0.1–0.2% at all temperatures (Table 1). The results from the frozen octanol experiments were not included in the quantum yield analysis but are described in *SI Appendix*, Fig. S6.

The spectra observed during photolysis of 24-DNP in acidified water are shown in Fig. 1*B*. The photolysis rate constants and quantum yields are listed in Table 2. The photolysis in water is more than two orders of magnitude slower than in octanol; no significant changes in the absorption spectra are detected even after 2 h of photolysis. The effective quantum yield of photolysis is only ~4 × 10^{-6}, the result that is consistent with previous observations of very slow aqueous photolysis of 24-DNP and other nitrophenols (25, 27, 28).

Table 1. Rate constants obtained from fitting the time-dependent 290-nm absorbance during photolysis of 24-DNP in octanol and in SOM to Eq. 1 at different temperatures

T, °C	k in octanol, × 10^{-4} s^{-1}	Quantum yield in octanol, × 10^{-3}	k in SOM, × 10^{-4} s^{-1}
25	2.20(1)	1.6	5.77(5)
25	2.04(1)	2.0	4.73(8)
25	2.55(1)	1.7	—
20	—	—	2.85(1)
20	—	—	2.48(4)
15	1.64(1)	1.3	1.77(2)
15	1.74(1)	1.4	2.03(2)
15	2.59(1)	1.5	
10	1.78(1)	1.8	1.56(1)
10	2.02(1)	1.2	0.99(1)
10	2.36(1)	1.1	
5	1.48(1)	1.4	0.89(1)
5	1.80(1)	1.2	0.90(1)
5	1.48(1)	1.6	
0	1.77(1)	1.3	0.64(1)
0	1.48(1)	1.7	0.73(1)
−10	1.23(1)	—	—
−10	1.01(1)	—	—
−17	1.13(1)	—	—
−17	1.07(2)	—	—
−18 (solid)	4.38(3)	—	—
−18 (solid)	5.58(3)	—	—

The errors in parentheses correspond to 1 SD in the fitted rate constants. Quantum yield values for 24-DNP/octanol are not included below −10 °C because of the uncertainty in the mechanism of photolysis of the azoxybenzene actinometer at lower temperatures. The sudden increase in the apparent rate constant in solid octanol at −18 °C is likely due to a change in the photolysis mechanism as discussed in *SI Appendix*.

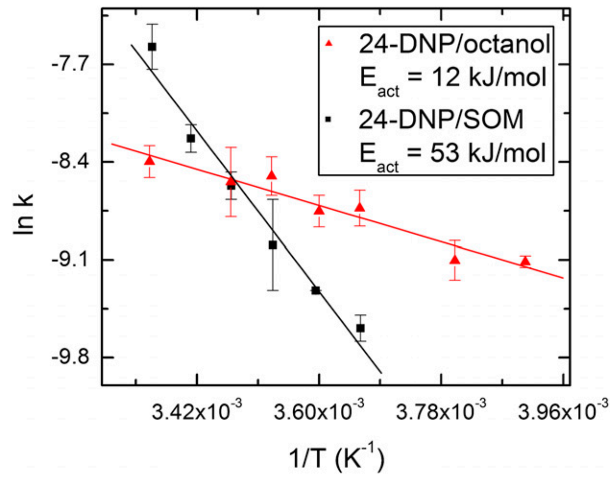

Fig. 2. Arrhenius plots for the 24-DNP photolysis in SOM matrix and in octanol. The point corresponding to the frozen octanol is omitted from the plot. The points are averaged values of different experiments at each temperature (Table 1). Activation energies are calculated from the linear fits to the ln(k) vs. 1/T data. The unexpectedly large activation energy for the SOM environment is the basis for our hypothesis that increased viscosity of SOM at lower temperature effectively arrests photochemistry of 24-DNP.

The absorption spectra recorded at different stages of photolysis of 24-DNP/SOM films at 25 °C are shown in Fig. 1*C*. As pointed out in *SI Appendix*, 24-DNP in SOM is found predominantly in a molecular form (*SI Appendix*, Fig. S7), which absorbs around 290 nm. The molar extinction coefficient of 24-DNP is also known to change with the solvent, and this was taken into account in the quantum yield calculations (*SI Appendix*, Fig. S8). The 24-DNP absorption features in the SOM film are not as well defined as they are in octanol or water because SOM compounds also absorb in the same spectral window; however, the 290-nm band can still be clearly discerned in the spectra. The absorbance due to the SOM itself does not change significantly during photolysis on the timescale of our experiments (as explicitly verified in separate control tests), whereas the 24-DNP absorbance at 290 nm decays exponentially as shown in Fig. 1*C*, *Inset*. An approximate isosbestic point at 330 nm and an increase in the 400-nm absorbance upon photolysis in both 24-DNP/SOM and 24-DNP/octanol experiments suggest that the mechanism of photolysis is qualitatively the same for these two types of organic films.

The observed 290-nm absorbance decay rates were fitted to Eq. **1** to get the corresponding photolysis rate constants, k, for 24-DNP. The expected first-order exponential decay to an asymptotic state was clearly observed at room temperature and still detectable at 10 °C, but as the temperature was lowered further, the photolysis became too slow to independently determine parameters β and k in Eq. **1**. Indeed, in the limit of small kt, Eq. **1** reduces to:

$$\frac{A(t)}{A_0} = 1 - k(1-\beta)t \qquad [3]$$

and only the product of k and $(1 - \beta)$ can be determined from a linear fit to Eq. **3**. The physical changes in the film, specifically the formation of "islands" shown in *SI Appendix*, Fig. S1, prevented us from extending the photolysis time beyond 2 h. To reduce the correlation between β and k, the parameter β was

Table 2. Rate constants obtained from fitting the time-dependent 290-nm absorbance during photolysis of 24-DNP in water to Eq. 1

T, °C	k, × 10^{-6} s^{-1}	Quantum yield, × 10^{-6}
20	0.95(7)	3.6
20	1.11(22)	4.4

The corresponding quantum yields are small, in agreement with known slow photodegradation of nitrophenols in water. The errors in parentheses correspond to 1 SD in the fitted rate constants.

fixed in Eq. **1** to the average value of 6.67 obtained from experiments at temperatures above 10 °C. Fixing the value of β requires that the 290-nm extinction coefficients of 24-DNP and its photolysis product must not vary significantly with temperature. The lack of significant temperature dependence was explicitly verified for 24-DNP by recording its absorption spectra in octanol at different temperatures (*SI Appendix*, Fig. S9). We also verified that the absorption spectra of the 24-DNP photolysis products are temperature independent; the measured product absorbance around 390 nm after 90 min photolysis did not change (<5% of the peak absorbance) in the temperature range from 0 °C to 25 °C. The resulting fitted values of k from all of the 24-DNP/SOM photolysis experiments are listed in Table 1 as a function of temperature and plotted in Fig. 2 in an Arrhenius plot.

One caveat of our analysis of the 24-DNP/SOM data is that Eq. **1** is valid only for optically thin substrates, requiring that absorbance must be <<1 for the photolyzing radiation from the UV lamp. Although this requirement is relatively well fulfilled in the 24-DNP/octanol experiments, Fig. 1*C* suggests that this limit does not strictly apply in the case of the 24-DNP/SOM experiments. Our repeated attempts to reduce the 24-DNP/SOM film thickness and to experiment with other ways of film preparation were unsuccessful; although a thinner film could be prepared, its lifetime with respect to "island formation" was still too short for performing meaningful photolysis experiments. Therefore, no quantum yields are reported in Table 1 for the 24-DNP/SOM experiments. The rates calculated using the above model can, however, be used to qualitatively compare the efficiency of the photolysis as a function of temperature even though quantitative determination of the photolysis quantum yields is not possible.

Atmospheric Implications. The time-dependent 24-DNP photolysis experiments carried out in different matrices reveal rich photochemical behavior, influenced both by the type of the matrix (liquid octanol, solid octanol, liquid or solid SOM, water) and by the temperature. Table 3 summarizes the findings and conclusions about the photolysis rates in different environments and at different temperatures.

There are two important conclusions arising from the current work. First, 24-DNP shows great enhancement in the photolysis efficiency upon moving from water to an organic environment. The atmospheric implication of this result is that 24-DNP and presumably other nitro-aromatic compounds, which are well-known mutagens and carcinogens (31, 32), will be degraded by photolysis much more readily in organic particles than in water or in the gas phase. It also clearly suggests that, in general, photochemistry in organic aerosol particles may be a significant loss mechanism for particulate organics. This conclusion supports the observations of Fan et al. (33) that nitro-polycyclic aromatic compounds photodegrade much faster in sunlight when they are associated with combustion particles. The large disparity in the apparent photolysis rate in water vs. octanol can be accounted for by the known fact that the photochemistry of nitrobenzenes in solutions is primarily driven not by direct photolysis but by a hydrogen abstraction reaction from the solvent by the photoexcited nitrobenzene (34, 35). C-H bonds on alpha-carbon atoms in alcohols are much better hydrogen-atom donors than O-H bonds in water, making it possible to photoreduce nitrobenzenes in alcohol solvents all the way to the corresponding anilines. It certainly seems that the organic reaction media plays a key role in the photochemical process.

The second important finding is the difference in photochemical rates in physically different organic reaction media. The similarity of the absorption spectra of 24-DNP and its photolysis products in SOM and octanol suggests that the mechanism of photolysis is similar in both matrices. To better illustrate this similarity, *SI Appendix*, Fig. S2, shows the spectrum of pure α-pinene SOM, α-pinene SOM doped with 24-DNP, and their difference spectrum, which looks nearly identical to the spectrum of 24-DNP in octanol. However, the rate of 24-DNP photolysis in SOM at 25 °C is even higher than the rate of photolysis in octanol. This suggests that at room temperature, the multifunctional compounds in SOM are on average better hydrogen-atom donors than octanol. This can be expected if we recall that SOM compounds commonly include species that contain hydroxyl groups attached to secondary carbon atoms, which serve as better hydrogen-atom donors compared with the C-H bonds in primary alcohols such as 1-octanol. For instance, the 313-nm quantum yield for the photoreduction of *p*-nitrobenzonitrile in isopropanol ($\phi = 0.48$) is nearly five times greater than that in ethanol at room temperature ($\phi = 0.11$) (34). In addition, SOM compounds may include other types of weakly bound hydrogen atoms provided by aldehydic and allylic C-H bonds.

The difference in the temperature dependence of the 24-DNP photodegradation rates in octanol and in SOM is striking (Fig. 2). Reducing the temperature in octanol causes only a relatively slight reduction in the photolysis rate. In contrast, the photolysis rate of 24-DNP embedded in SOM is significantly suppressed at reduced temperatures, by nearly an order of magnitude between 25 °C and 0 °C. The Arrhenius equation describes the photolysis behavior of both systems quite well (Fig. 2); the effective activation energies obtained from the Arrhenius fits to the rates of 24-DNP/SOM and 24-DNP/octanol photolysis are 53 kJ/mol and 12 kJ/mol, respectively. As mentioned above, the hydrogen-atom abstraction by 24-DNP from SOM compounds should be more facile than that from octanol, and if anything, one should expect the opposite trend in the activation energies. We hypothesize, based on the following arguments, that large difference in the apparent activation energies can be ascribed to the temperature-dependent changes in the viscosity of the surrounding matrices. The viscosity of octanol is 7.3 mPa·s at room temperature, and it is expected to increase by less than an order of magnitude based on the extrapolation of data from ref. 36 to temperature of −10 °C. This is in accordance with the slight temperature-dependent trend observed in the Arrhenius plot. In stark contrast to this, the SOM formed by ozonolysis of α-pinene may have viscosity in excess of 10^3 Pa·s (37) in the humidity range at which the SOM films were prepared [~50–60% relative humidity (RH) in the laboratory air]. As the known products of α-pinene oxidation such as *cis*-pinonic acid and pinic acid undergo glass transitions at low temperatures (3), the α-pinene SOM can similarly be expected to glassify upon sufficient cooling. It is plausible that the phase state gradually changes at reduced temperatures and arrests the molecular motion to the extent that photoexcited 24-DNP is unable to readily abstract a hydrogen atom from surrounding SOM molecules, and instead loses its energy thermally. Indeed, the hydrogen atom abstraction requires the proximity between the $-NO_2$ group in 24-DNP and a weak C-H bond in a SOM compound, which may be difficult to achieve when librational and diffusional motion in the organic matrix is constrained. It should be noted that based on the estimated glass transition temperatures of α-pinene SOM components by Koop et al. (3), it can be assumed that the actual glass transition temperature of the α-pinene SOM is not reached

Table 3. Summary of the observations of photochemistry of 24-DNP dispersed in matrixes with varying viscosity and temperature

Matrix	Characteristics	24-DNP photolysis rate	Effect of temperature on the 24-DNP photolysis rate
Water	liquid	very slow	not investigated
Octanol	viscous organic liquid	fast	slight reduction at lower temperature
SOA	highly viscous organic liquid (or solid)	fast	significant reduction at lower temperature

in our experiments, and the observed kinetic behavior is not a result of a sudden phase change but of the gradually increasing viscosity of the organic matrix.

The relationship between viscosity changes as a function of temperature and Arrhenius behavior in photochemical reactions has been previously discussed in the context of cyanine dyes (38). It was found that the rates of photochemical reactions with low intrinsic activation energies are mainly controlled by viscosity effects. In other words, the apparent slope in the Arrhenius plot is controlled by matrix constraints and not by the energetics of the photochemical reaction itself. The viscosity control can be inferred from a comparison between the Arrhenius slope of the photochemical reaction rate and from that of the viscosity coefficient of the solvent. For the viscosity-controlled reactions, the two Arrhenius slopes should be comparable. Conversely, for reactions with high intrinsic activation energies, the reaction rate Arrhenius slope should be much larger than that for the viscosity coefficient (38). In the present work, the extrapolated viscosity Arrhenius curves for octanol and SOM correlate relatively well with the corresponding reaction rate Arrhenius slopes. The normalized viscosity Arrhenius slopes ($S_V = \ln \eta$ vs. 1,000/T, where T is absolute temperature) and the photolysis rate Arrhenius slopes ($S_P = \ln k$ vs. 1,000/T) compare in the following way for the two organic matrices: $S_V = 3.4$ K and $S_P = 1.4$ K for octanol; $S_V = 23.5$ K and $S_P = 6.4$ K for SOM (details for the slope estimations can be found in *SI Appendix*). The large value for the viscosity slope ($S_V > S_P$) provides indirect evidence for the viscosity-controlled mechanism. Furthermore, the large value for S_V in SOM is consistent with more significant viscosity effects in that matrix.

Although the SOM viscosity enhancement upon cooling provides an attractive explanation for the observed steep reduction in the rate of photolysis of 24-DNP, the possibility of change in the reaction mechanism between the SOM and octanol environments cannot be ruled out. SOM compounds contain other reactive functional groups permitting hydrogen-atom abstraction, such as aldehydes and peroxides (39–41). Other possibilities not discussed here, such as energy transfer, electron transfer, and production of singlet oxygen, cannot be completely excluded without further confirmation. To unambiguously confirm the viscosity-based explanation, a detailed product analysis of 24-DNP photolysis in SOM is needed, something that is beyond our current experimental capabilities due to the small amounts of material in the 24-DNP/SOM film. In addition, future experiments should thoroughly compare photochemistry of 24-DNP/SOM under conditions when SOM viscosity is controlled not only by lowering the system temperature, as done in this work, but also by lowering ambient relative humidity, as done in ref. 37. We have carried out preliminary room-temperature experiments on 24-DNP/SOM films where the RH was the control variable (instead of the temperature) for varying the SOM rheological properties. The effect of RH on the photolysis rate of 24-DNP is shown in *SI Appendix*, Fig. S5. Making the SOM film more viscous by extensive (many hours) drying at room temperature slows down the rate of 24-DNP photodegradation by about a factor of 2 compared with the experiments in SOM at elevated RH. This observation lends strong support to the conclusion derived from the temperature-controlled experiments presented in this work that SOM viscosity affects 24-DNP photochemistry. We want to point out that the experiments in which the viscosity is varied by controlling humidity are considerably more time-consuming as complete dehydration and humidification of SOM takes a very long time (7). It should also be noted that the humidity-controlled experiments are harder to reproduce, suggesting that temperature control is the preferred method for this type of experiments. Finally, we note that SOM films containing residual water may exhibit rather complicated behavior upon cooling such as freeze-drying followed by glassification and morphology change, as described by Adler et al. (42).

Results of this work contribute to the growing body of evidence that the phase state of aerosol particles has a significant effect on their physical and chemical properties. Although it is not possible to fully confirm the viscosity-dependent deceleration of photochemical reactions without further product identification, this study clearly demonstrates the importance of the reaction media in photochemical processes taking place in atmospheric aerosol particles. It also highlights the complexity of interpreting the underlying mechanisms of atmospheric aerosol photochemistry, as they are strongly dependent on both temperature and relative humidity. It is already established that the glassy, highly viscous state of aerosol particles can influence the gas–particle partitioning of semivolatile compounds, reduce the rate of heterogeneous chemical reactions, affect water uptake, and change the atmospheric lifetimes of compounds in particles with respect to OH and O_3 oxidation (3, 8, 17, 43–45). The reduced reaction rates due to viscosity in general are not an unknown phenomenon; a termination of polymerization at an ultraviscous threshold as an example (46). The experimental results presented in this paper strongly suggest that photolysis reactions could also be affected by the particle viscosity, which has significant implications for understanding the mechanisms of photochemical aging and interpreting atmospheric lifetimes of particle-associated organics. For example, stabilization of organic compounds with respect to photolytic loss by viscosity effects could explain the unexpected occurrence of long-lived oxidized organics in the stratospheric particles recently observed by in situ single-particle mass spectrometry measurements (47).

Materials and Methods

The methods used in this study are briefly presented below, and a considerably more detailed description is provided in *SI Appendix*. SOM was produced by oxidizing α-pinene with O_3 without seed particles in a flow reactor (48) and collected on a CaF_2 window using a Sioutas impactor (49). One of the novel aspects of this study is the use of a suitable photochemical probe molecule (24-DNP) embedded into the SOM matrix as an indicator of the effects of temperature and viscosity on the aerosol photochemistry. The method that appeared to work best for dispersing 24-DNP throughout the SOM matrix involved adding a 100-μL droplet of solution containing a known amount of 24-DNP in methanol to the CaF_2 window that contained a known amount of SOM material. The SOM was dissolved, and the methanol was allowed to evaporate in open air (typical relative humidity ~50%). The film was then tightly sandwiched between two identical CaF_2 windows (*SI Appendix*, Fig. S1). Because of the sandwiching, the film likely retained residual water and methanol during the experiments even though the photolysis compartment was purged with dry air to prevent water condensation on the outer surfaces of the windows. A typical 24-DNP:SOM mass ratio was 1:50. The 24-DNP/octanol films were prepared by placing a 15-μL droplet of 24-DNP/octanol solution between two CaF_2 windows. The films were photolyzed in a setup (*SI Appendix*, Fig. S3) designed for variable temperature film photochemistry experiments (50) and monitored using UV-visible (UV-vis) spectroscopy. The 24-DNP/water samples were photolyzed in a constant temperature cell holder inside a UV-vis spectrometer.

SI Appendix contains a detailed description of the materials and methods used in this study, a description of the results of photolysis experiments at different RH, a description of the results of photolysis of 24-DNP in frozen octanol, a discussion of the acid-base equilibrium of 24-DNP in SOM and octanol films, and a description of how the temperature-dependent viscosity of octanol and SOM was estimated.

ACKNOWLEDGMENTS. Dr. Scott Epstein is thanked for many helpful comments and acknowledged for the design of the solid-state photolysis setup. Dr. Carla Kidd is warmly acknowledged for fruitful discussions. Funding from National Science Foundation Grants AGS-1227579 (to S.A.N.) and CHE-0909227 (to H.L. and M.L.H.) are acknowledged. H.L. also acknowledges the Finnish Cultural Foundation and Magnus Ehrnrooth Foundation for financial support.

1. Ravishankara AR, Longfellow CA (1999) Reactions on tropospheric condensed matter. *Phys Chem Chem Phys* 1(24):5433–5441.
2. Ervens B, Turpin BJ, Weber RJ (2011) Secondary organic aerosol formation in cloud droplets and aqueous particles (aqSOA): A review of laboratory, field and model studies. *Atmos Chem Phys* 11(21):11069–11102.
3. Koop T, Bookhold J, Shiraiwa M, Pöschl U (2011) Glass transition and phase state of organic compounds: Dependency on molecular properties and implications for secondary organic aerosols in the atmosphere. *Phys Chem Chem Phys* 13(43):19238–19255.
4. Abramson E, Imre D, Beránek J, Wilson J, Zelenyuk A (2013) Experimental determination of chemical diffusion within secondary organic aerosol particles. *Phys Chem Chem Phys* 15(8):2983–2991.
5. Perraud V, et al. (2012) Nonequilibrium atmospheric secondary organic aerosol formation and growth. *Proc Natl Acad Sci USA* 109(8):2836–2841.
6. Vaden TD, Imre D, Beránek J, Shrivastava M, Zelenyuk A (2011) Evaporation kinetics and phase of laboratory and ambient secondary organic aerosol. *Proc Natl Acad Sci USA* 108(6):2190–2195.
7. Bones DL, Reid JP, Lienhard DM, Krieger UK (2012) Comparing the mechanism of water condensation and evaporation in glassy aerosol. *Proc Natl Acad Sci USA* 109(29):11613–11618.
8. Shiraiwa M, Ammann M, Koop T, Pöschl U (2011) Gas uptake and chemical aging of semisolid organic aerosol particles. *Proc Natl Acad Sci USA* 108(27):11003–11008.
9. Power RM, Simpson SH, Reid JP, Hudson AJ (2013) The transition from liquid to solid-like behaviour in ultrahigh viscosity aerosol particles. *Chem. Sci* 4(6):2597–2604.
10. Hearn JD, Smith GD (2005) Measuring rates of reaction in supercooled organic particles with implications for atmospheric aerosol. *Phys Chem Chem Phys* 7(13):2549–2551.
11. Knopf DA, Anthony LM, Bertram AK (2005) Reactive uptake of O_3 by multicomponent and multiphase mixtures containing oleic acid. *J Phys Chem A* 109(25):5579–5589.
12. Shiraiwa M, et al. (2013) Size distribution dynamics reveal particle-phase chemistry in organic aerosol formation. *Proc Natl Acad Sci USA* 110(29):11746–11750.
13. Kidd C, Perraud V, Wingen LM, Finlayson-Pitts BJ (2014) Integrating phase and composition of secondary organic aerosol from the ozonolysis of α-pinene. *Proc Natl Acad Sci USA* 111(21):7552–7557.
14. Pankow JF (1994) An absorption model of gas/particle partitioning of organic compounds in the atmosphere. *Atmos Environ* 28(2):185–188.
15. Pankow JF (1994) An absorption model of the gas/aerosol partitioning involved in the formation of secondary organic aerosol. *Atmos Environ* 28(2):189–193.
16. Odum JR, et al. (1996) Gas/particle partitioning and secondary organic aerosol yields. *Environ Sci Technol* 30(8):2580–2585.
17. Shiraiwa M, Seinfeld JH (2012) Equilibration timescale of atmospheric secondary organic aerosol partitioning. *Geophys Res Lett* 39(24):L24801.
18. Virtanen A, et al. (2010) An amorphous solid state of biogenic secondary organic aerosol particles. *Nature* 467(7317):824–827.
19. McDow SR, Jang M, Hong Y, Kamens RM (1996) An approach to studying the effect of organic composition on atmospheric aerosol photochemistry. *J Geophys Res* 101(D14): 19593–19600.
20. Sangster J (1989) Octanol-water partition coefficients of simple organic compounds. *J Phys Chem Ref Data* 18(3):1111–1229.
21. Shea PJ, Weber JB, Overcash MR (1983) Biological activities of 2,4-dinitrophenol in plant-soil systems. *Residue Rev* 87:1–41.
22. Harris MO, Corcoran JJ (1995) *Toxicological Profile for Dinitrophenols* (US Department of Human and Health Services, Washington, DC).
23. Sanagi MM, Miskam M, Wan Ibrahim WA, Hermawan D, Aboul-Enein HY (2010) Determination of partition coefficient and analysis of nitrophenols by three-phase liquid-phase microextraction coupled with capillary electrophoresis. *J Sep Sci* 33(14): 2131–2139.
24. Desyaterik Y, et al. (2013) Speciation of "brown" carbon in cloud water impacted by agricultural biomass burning in eastern China. *J Geophys Res* 118(13):7389–7399.
25. Albinet A, Minero C, Vione D (2010) Phototransformation processes of 2,4-dinitrophenol, relevant to atmospheric water droplets. *Chemosphere* 80(7):753–758.
26. Yang G-P, Qi J-L (2002) Studies on photochemical oxidation of nitrophenols in seawater. *Chem. J. Chinese Univ.* 23(6):1180–1182.
27. Lipczynska-Kochany E (1992) Degradation of nitrobenzene and nitrophenols in homogeneous aqueous solution. Direct photolysis versus photolysis in the precence of hydrogen peroxide and the Fenton reagent. *Water Pollut Res J Can* 27(1):97–122.
28. Alif A, Pilichowski J-F, Boule P (1991) Photochemistry and environment XIII: Phototransformation of 2-nitrophenol in aqueous solution. *J Photochem Photobiol Chem* 59(2):209–219.
29. Bejan I, et al. (2006) The photolysis of ortho-nitrophenols: A new gas phase source of HONO. *Phys Chem Chem Phys* 8(17):2028–2035.
30. Lignell H, et al. (2013) Experimental and theoretical study of aqueous *cis*-pinonic acid photolysis. *J Phys Chem A* 117(48):12930–12945.
31. Pitts JN, Jr, et al. (1978) Atmospheric reactions of polycyclic aromatic hydrocarbons: Facile formation of mutagenic nitro derivatives. *Science* 202(4367):515–519.
32. Finlayson-Pitts BJ, Pitts JN, Jr (2000) *Chemistry of the Upper and Lower Atmosphere: Theory, Experiments and Applications* (Academic, London).
33. Fan Z, Kamens RM, Hu J, Zhang J, McDow S (1996) Photostability of nitro-polycyclic aromatic hydrocarbons on combustion soot particles in sunlight. *Environ Sci Technol* 30(4):1358–1364.
34. Hashimoto S, Kano K (1972) The photochemical reduction of nitrobenzene and its reduction intermediates. X. The photochemical reduction of the monosubstituted nitrobenzenes in 2-propanol. *Bull Chem Soc Jpn* 45(2):549–553.8.
35. Barltrop JA, Bunce NJ (1968) Organic photochemistry. Part VIII. The photochemical reduction of nitro-compounds. *J Chem Soc C* 1968:1467–1474.
36. França Faria MA, et al. (2005) Measurement of density and viscosity of binary 1-alkanol systems (C8–C11) at 101 kPa and temperatures from (283.15 to 313.15) K. *J Chem Eng Data* 50(6):1938–1943.
37. Renbaum-Wolff L, et al. (2013) Viscosity of α-pinene secondary organic material and implications for particle growth and reactivity. *Proc Natl Acad Sci USA* 110(20): 8014–8019.
38. Rettig W, Rurack K, Sczepan M (2001) From cyanines to styryl bases—Photophysical properties, photochemical mechanisms, and cation sensing abilities of charged and neutral polymethinic dyes. *New Trends in Fluorescence Spectroscopy*, eds Valeur B, Brochon J-C (Springer, Berlin), pp 125–155.
39. Yu J, et al. (1999) Gas-phase ozone oxidation of monoterpenes: Gaseous and particulate products. *J Atmos Chem* 34(2):207–258.
40. Jang M, Kamens RM (1999) Newly characterized products and composition of secondary aerosols from the reaction of α-pinene with ozone. *Atmos Environ* 33(3):459–474.
41. Jaoui M, Kamens RM (2003) Gaseous and particulate oxidation products analysis of a mixture of α-pinene + β-pinene/O_3/air in the absence of light and α-pinene + β-pinene/NO_x/air in the presence of natural sunlight. *J Atmos Chem* 44(3):259–297.
42. Adler G, et al. (2013) Formation of highly porous aerosol particles by atmospheric freeze-drying in ice clouds. *Proc Natl Acad Sci USA* 110(51):20414–20419.
43. Murray BJ (2008) Inhibition of ice crystallisation in highly viscous aqueous organic acid droplets. *Atmos Chem Phys* 8(17):5423–5433.
44. Mikhailov E, Vlasenko S, Martin ST, Koop T, Pöschl U (2009) Amorphous and crystalline aerosol particles interacting with water vapor: Conceptual framework and experimental evidence for restructuring, phase transitions and kinetic limitations. *Atmos Chem Phys* 9(24):9491–9522.
45. Pfrang C, Shiraiwa M, Pöschl U (2011) Chemical ageing and transformation of diffusivity in semi-solid multi-component organic aerosol particles. *Atmos Chem Phys* 11(14):7343–7354.
46. Odian G (2004) *Principles of Polymerization* (Wiley, New York), 4th Ed.
47. Murphy DM, Froyd KD, Schwarz JP, Wilson JC (2013) Observations of the chemical composition of stratospheric aerosol particles. *Q J R Meteorol Soc* 140(681):1269–1278.
48. Updyke KM, Nguyen TB, Nizkorodov SA (2012) Formation of brown carbon via reactions of ammonia with secondary organic aerosols from biogenic and anthropogenic precursors. *Atmos Environ* 63:22–31.
49. Sioutas C (2004) US Patent 6,786,105 B1.
50. Epstein SA, Shemesh D, Tran VT, Nizkorodov SA, Gerber RB (2012) Absorption spectra and photolysis of methyl peroxide in liquid and frozen water. *J Phys Chem A* 116(24): 6068–6077.